Molecular Determinants of Liquid-liquid Phase Separation of an Intrinsically Disordered Protein

Shiny Maity

A dissertation submitted for the partial fulfilment of

BS-MS dual degree in Science

Department of Chemical Sciences

Indian Institute of Science Education and Research (IISER) Mohali

April 2019

Certificate of Examination

This is to certify that the dissertation titled "Molecular Determinants of Liquid-liquid Phase Separation of an Intrinsically Disordered Protein" submitted by Ms. Shiny Maity (MS14113) for the partial fulfilment of BS-MS dual degree programme of the Institute, has been examined by the thesis committee duly appointed by the Institute. The committee finds the work done by the candidate satisfactory and recommends that the report be accepted.

Dr. Sabyasachi Rakshit Dr. Angshuman Roychoudhury Dr. Samrat Mukhopadhyay

(Supervisor)

Declaration

The work presented in this dissertation has been carried out by me under the supervision of Dr. Samrat Mukhopadhyay at the Department of Chemical Sciences, Indian Institute of Science Education and Research (IISER) Mohali.

This work has not been submitted in part or full for a degree, a diploma, or a fellowship to any other university or institute.

Whenever contributions of others are involved, every effort is made to indicate this clearly, with due acknowledgement of collaborative research and discussions. This thesis is a bona fide record of original work done by me and all sources listed within have been detailed in the bibliography.

Date Shiny Maity

In my capacity as supervisor of the candidate's thesis work, I certify that the above statements by the candidate are true to the best of my knowledge.

Dr. Samrat Mukhopadhyay

(Supervisor)

Acknowledgements

I would like to express sincere gratitude to my supervisor Dr. Samrat Mukhopadhyay for his relentless guidance, encouragement and support throughout my research. The thing which I truly like about him is his great depth of knowledge about his area of research. His passion for scientific research is a real inspiration to all in the lab. He always says that "experiments do not work, we have to make them work" instils an immense urge in us to work harder and stay motivated when things do not work out. He has not only provided us with a good scientific environment with the state-of-the-art techniques but has also provided us with the opportunity to interact with some of the best scientists in the field. He puts an enormous amount of effort in shaping our scientific outlook and takes care of every detail related to our academic and personal development.

My project would have been almost impossible without the guidance of Dr. Anupa Majumdar. I am grateful to her for teaching me the basics of all the biophysical tools that I have utilized in this project, for providing me personal attention and help me come up with ideas to troubleshoot various problems while conducting experiments. She has played a huge role in executing my scientific thoughts and helped me with all the experiments. I would also like to thank her for recording time-resolved anisotropy decays of fluorescein-labeled tau K18 which was an important part of the project. I am thankful to her for her intellectual inputs and critical comments which has given the project a new horizon. Besides being a critical scientist, she is an amazing person as well. I truly acknowledge her for going through my thesis and presentations meticulously and cheering me up during my tough times.

I thank Priyanka Dogra for training me during the initial days of my tenure. I owe to her for all the knowledge I have in protein expression and purification and appreciate her painstaking effort in providing me with a hand-on experience in molecular biology.

I am grateful to all the members of The Mukhopadhyay Lab for their constant encouragement and fruitful discussions for the scientific improvement of my work. My tenure would have been tougher and longer without their presence. I enjoyed working with all of them, including Debopriya, Aishwariya, Sayanta, Priyanka M, Priyanka D, Anupa,

Swapnil, Anamika, Sandeep. I had an amazing time working with Achuthan during the summer break. I owe special thanks to Ashish and Lisha for their enthusiasm and cordiality which made my stay more memorable.

I would like to thank the members of my ms thesis committee, Dr. Sabyasachi Rakshit and Dr. Angshuman RoyChoudhury for their critical comments and valuable suggestions on my work.

I would like to acknowledge Prof. Elizabeth Rhodes, Associate Professor of Chemistry, University of Pennsylvania, for providing us with tau K18 plasmids and Prof. N. Periasamy (Retd. TIFR Mumbai) for providing a decay analysis program for analyzing the time-resolved fluorescence data. I am grateful to IISER Mohali and Centre for Protein Science, Design and Engineering for providing all the facilities for research. I would like to express my sincere gratitude to the Department of Science and Technology, Govt. of India, for the DST-INSPIRE fellowship.

I am thankful for the constant support of my friends Swetha, Darsana, Greeshma, Sachin, Priyasha, Somak, Adarsh, Varun, and Vishnu. I enjoyed my time in the maths room with Swetha, Sachin and Somak. I would always be grateful to Swetha, Darsana and Greeshma for their love, care and support. I enjoyed my long refreshing coffee breaks and mid-night snacks with Priyasha and Adarsh. My special thanks to Priyasha who was the most wonderful labmate I ever had and was always with me during my difficult times. She never failed to encourage me and was always a constant source of inspiration for me.

Last but not the least, I am grateful to my parents for their constant love and encouragement. The journey would have been impossible without their constant moral support.

List of Figures

Figure 11. (a) Changes in turbidity in the monomer and droplet state of tau K18 with increasing concentrations of NaCl, measured at 350 nm. (b) Changes in the steady-state anisotropy in the monomer and droplet state of tau K18 with increasing concentrations of NaCl.

Figure 12. (a) Schematic representation of the local motion of a dye molecule and the global tumbling of the protein. (b) Schematic representation of the global motion of a compact globule and the torsional mobility of the polypeptide backbone. (Image courtesy: Dr. Anupa Majumdar and Dr. Samrat Mukhopadhyay)

Figure 13. (a) Time-resolved fluorescence anisotropy decays. The black lines are the fits using bi-exponential decay kinetics of depolarization. (b) Changes in rotational correlation times along with the standard deviation for three independent measurements. (All time-resolved anisotropy experiments were performed and the data were analyzed by Dr. Anupa Majumdar, a National Post-Doctoral Fellow in our lab.)

List of Tables

Contents

Molecular Determinants of Liquid-liquid Phase Separation of an Intrinsically Disordered Protein

Shiny Maity

Department of Chemical Sciences

Indian Institute of Science Education and Research (IISER), Mohali

M.S. Thesis Supervisor: Dr. Samrat Mukhopadhyay

ABSTRACT:

Liquid-liquid phase separation has recently been recognized as a new principle by which membrane-less intracellular compartments are formed.[1-5] These cellular bodies are composed of non-stoichiometric assemblies of thousands of different protein and nucleic acids which segregate themselves from the surrounding cytoplasm to form complex-coacervates. Intrinsically disordered multivalent proteins with low complexity domains have been found to be the drivers of phase separation.[6-11] The intrinsically disordered regions (IDRs) act as highly dynamic linkers and promote "fuzzy" interactions between the repetitive interaction domains in a variety of combinations.[12] However, the molecular origin of liquid-liquid phase separation remains unknown. Here, we demonstrate the change in the conformational landscape and the associated chain dynamics of an intrinsically disordered protein, tau k18, in the protein-rich de-mixed phase, utilizing an array of biophysical tools. Using an intramolecular proximity readout, we show that tau k18 undergoes conformational expansion which enables it to form intermolecular cross-talks between the polypeptide chains upon phase separation. We also demonstrate that these phase-separated proteinaceous droplets are not water excluded and the polypeptide chains experience significant chain solvation with the help of Stern-Volmer quenching experiments. Using time-resolved fluorescence anisotropy measurements we reveal that the polypeptide chain dynamics increases inside the protein droplets indicating rapid conformational fluctuations which enable weak, transient intermolecular interactions between the "sticky" domains of the polypeptide chains. Such polypeptide chain fluctuations are of crucial importance as they help in maintaining the liquid-like nature of the condensates. In summary, our results, together with conformational expansion and extensive conformational dynamics during phase separation facilitate transient intermolecular interaction, thus promoting liquid-liquid phase separation.

1. INTRODUCTION:

A novel class of proteins known as the intrinsically disordered proteins (IDPs) despite being biologically active, defies the traditional sequence-structure-function relationship. Unlike globular protein, IDPs lack a single three-dimensional structure and have a shallow free-energy surface.[13] They are intrinsically disordered, that is they have an inherent tendency to remain in a disordered state. This is mainly due to their preference for disorder-promoting amino acids like Ala, Arg, Gly, Gln, Ser, Glu, Lys, Pro which provide them with low mean hydrophobicity and high net charge, that in turn deter them from having compactness in their structures.[14] Being conformationally plastic, they can bind to multiple binding partners and thus exhibit multi-functionality.[14] Recently IDPs have drawn the attention of various scientists due to their implications in various debilitating diseases. Since they are disordered in their native state, they are prone to misfolding which forms the basis of various neurodegenerative diseases like Parkinson's[15], Alzheimer's[16], Huntington's[18], Amyotrophic lateral sclerosis (ALS)[17], Frontotemporal dementia (FTD)[17], etc.

Many disordered proteins involved in neurodegeneration have a propensity to undergo phase separation to highly condensed liquid droplets. Phase separation as the name suggests is the separation of a homogeneous solution of macromolecules into two coexisting liquid phases, one rich in macromolecules and the other depleted in these molecules.[19-21] Phase separation has recently been thought of as a phenomenon by which cells organize thousands of different proteins and nucleic acids into several compartments which are membrane-less.[1-5] These membrane-less organelles are enriched in proteins and RNA.[23] They segregate from the rest of the cytoplasm due to increase in concentration or change in the surrounding environment (e.g., Temperature, pH, etc.) and form protein-rich viscous droplets that have liquid-like properties.[2] These droplets are spherical in nature which helps them to reduce the surface tension.[2] They drip and flow on application of stress and also fuse when the droplets come in contact with each other.[2] Intrinsically disordered proteins with low complexity domains have been found to be the predominant drivers of phase separation.[6-11] Disordered multivalent proteins with blocks of alternating positive and negative charges enable the polypeptide chains to undergo electrostatic and short-range interactions like cation-π, π-π stacking, dipole-dipole interactions, etc.[22] Proteins undergoing phase separation have also been considered as biological associative polymers, characterized by

multivalent interaction domains, called the "stickers", which are interspersed by dynamic linkers or "spacers".[9,24] Intrinsically disordered regions (IDRs) serve as the spacers, that help to promote weak, non-covalent, transient interactions between the sticky domains and thus help in determining the material property of the phase separated droplets.[9,24]

Though intense scientific research has been carried out on liquid-liquid phase separation of various proteins and nucleic acids, the molecular mechanism of phase separation remains elusive. Here, in our work, with the help of sensitive optical probes, we directly observe the conformational expansion, solvation, and fluctuations during the course of phase separation. We chose to work with the K18 fragment of the tau protein, an IDP, whose misfolding is a precursor to the infamous neurological disease, Alzheimer's.[25-28] Tau is primarily found in the central nervous system, and its principal function is to bind to the microtubules and promote their assembly.[28] There are six isoforms of tau found in the human brain which arise due to the alternative splicing of the pre-mRNA. In the longest isoform, both the N-terminus, also called the 'projection domain' and the C-terminus are negatively charged.[28] The central domain, known as the 'microtubule binding domain' is predominantly positively charged and mainly comprises four imperfect repeats called R1, R2, R3, R4 (**Figure 1**).[28] For this work, we chose to work with the K18 fragment which consists of these four imperfect repeats, because they form the core of the microtubule binding domain and can modulate the ability of tau to undergo aggregation and form neurofibrillary tangles in Alzheimer's disease.[28] It has been shown that both full-length tau as well as tau k18 undergoes phase separation.[29-30] Phase separation of tau has functional as well as pathological role. Tau droplets play a functional role by promoting the formation of microtubule assembly.[31] It has been found that tau phase separates into liquid-like droplets under cellular crowding conditions and as soon as the droplets are formed, tubulin gets incorporated inside the droplets which facilitate the formation of microtubules.[31] Tau droplets also play a pathological role by acting as the initial step towards aggregation.[30] Upon hyperphosphorylation or in presence of FTD mutations, these dynamic and reversible tau droplets can serve as micro-reactors that can further seed irreversible, pathogenic aggregation.[30]

2. EXPERIMENTAL METHODS:

2.1 Materials

The chemicals used for preparing buffer solutions, such as, sodium phosphate monobasic dihydrate, Tris (2-carboxyethyl) phosphine hydrochloride (TCEP), MES (2-(N-Morpholino)ethanesulfonic acid hydrate, EDTA (Ethylenediaminetetraacetic acid), Magnesium chloride hexahydrate, DTT (DL-Dithiothreitol) were obtained from Sigma Aldrich (St. Louis, MO). All the fluorescent probes, namely, fluorescein-5-maleimide, N-(1-pyrene) maleimide, Acrylodan (6-Acryloyl-2-Dimethylaminonaphthalene), AlexaFluor 488 C5-maleimide, and AlexaFluor 594 C5-maleimide were purchased from Molecular Probes, Invitrogen. The free fluorescein dye was purchased from Fluka Analytical. SP Sepharose resin used for protein purification and PD-10 columns were purchased from GE Healthcare Life Sciences (USA). The protein concentrators and filters were procured from Merck Millipore. A Metrohm 827 lab pH meter was used to adjust the final pH (± 0.01) of all the buffer solutions prepared in Milli-Q water and filtered before use.

2.2 Protein Expression and Purification:

Tau k18 was expressed using recombinant DNA technology in Escherichia coli BL21(DE3) and purified using the procedure as mentioned previously with slight modification.[32] Briefly stating, using a lysis buffer of pH 8 (50 mM Tris, 150 mM NaCl, 10 mM EDTA), the cells were lysed by boiling it for half an hour at 100˚C. The lysate was then centrifuged at 11,500 rpm at 4˚C for 30 mins, following which the supernatant was treated with 136 µL/mL of 10% streptomycin sulfate and 228 µL/mL of glacial acetic acid for the precipitation of DNA. Next, it was further centrifuged at 11,500 rpm at 4˚C for 30 mins. The supernatant collected was then mixed with saturated ammonium sulfate and kept for 2-3 hrs for salting out of the protein. The protein pellet obtained upon centrifugation was washed with 100 mM ammonium acetate and 100% ethanol and kept for drying at 37˚C overnight. After 12-13 hrs, the dried pellet was dissolved in native buffer (20 mM MES, 1 mM EDTA, 2 mM DTT and 1 mM $MgCl_2$) of pH: 6.8 and purified using SP Sepharose column with the help of FPLC (Fast Protein Liquid Chromatography). The fractions collected were further dialyzed overnight using the native buffer (20 mM MES, 1 mM EDTA, 2 mM DTT and 1 mM $MgCl_2$) of pH 6.8, following which it was stored at -80˚C. The purity of the protein was analyzed by SDS-PAGE.

(a)

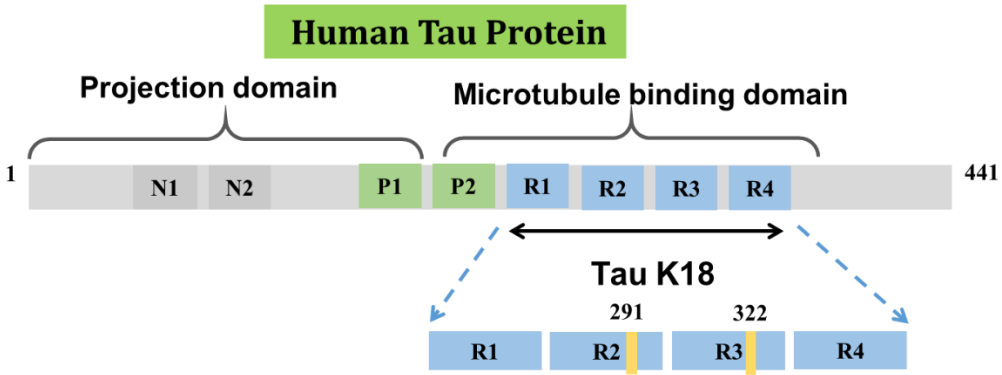

(b)

244 - QTAPVPMPDLK NVKSKIGSTENLKHQPGGGK R1
275 - VQIINKKLDLS NVQSKCGSKDNIKHVPGGGS R2
306 - VQIVYKPVDLS KVTSKCGSLGNIHHKPGGGQ R3
337 - VEVKSEKLDFKDRVQSKIGSLDNITHVPGGGN R4
369 - KKIE

Figure 1. (a) Different regions of full-length human tau protein, highlighting the four repeat domains which constitute the core of tau K18. The two native cysteines in tau K18 are represented by yellow bars. (b) The sequence of tau K18 showing the distribution of charged amino acids.

2.3 Fluorescence labeling of tau K18 with *N*-(1-pyrene) maleimide

The two native cysteine residues in tau k18 were covalently labeled under a denatured and reduced condition with a fluorescent probe, *N*-(1-pyrene) maleimide, utilizing its thiol reactivity. Initially, tau k18 was incubated in 6 M GdmCl (50 mM phosphate, 1 mM TCEP) buffer of pH 7 and kept overnight at 4˚C to ensure its complete denaturation. The denatured tau k18 was then mixed with a freshly prepared stock of 50 mM pyrene-maleimide solution (in DMSO) in the ratio 1:10:30 (tau k18: TCEP: dye) and the labeling reaction was conducted under constant stirring of 1500 rpm at 37˚C for 4hrs. After every 10 mins, 5 uL of 50 mM pyrene-maleimide was added to the reaction mixture to facilitate the higher probability of reaction. At the end of the reaction, tau k18 was eluted with 50 mM sodium

phosphate (0.5 mM TCEP) buffer of pH 8.8 using PD-10 column to remove the unreacted dye. The initial fractions of the eluted protein were pooled together, and the concentration of the labeled protein was calculated using a molar extinction coefficient of 40,000 M^{-1} cm^{-1} at 340 nm. The labeled protein was used in doping concentration (1%) for the experiments, to ensure that the observed excimer fluorescence was due to intramolecular interaction as opposed to intermolecular interaction.

2.4. Fluorescence labeling of tau K18 with other thiol-active fluorescent dyes

Taking advantage of the two native cysteines, tau k18 was reacted with thiol-reactive environment-sensitive probes, namely, fluorescein-5-maleimide (F-5-M) (0.5 equivalents), IAEDANS (1 equivalent), Acrylodan (2 equivalents), respectively in the native buffer (20 mM MES, 2 mM DTT, 1 mM MgCl2, 1 mM EDTA, pH 6.8) and the reaction mixture was stirred at room temperature at a speed of 6 rpm. After 3 hrs, the labeled protein was eluted using a PD-10 column with 50 mM sodium phosphate (0.5 mM TCEP) buffer of pH 8.8. The labeling efficiency was estimated by measuring the absorption of the labeled protein at the respective emission wavelengths of the fluorescent probes. For all the experiments, labeled protein was mixed with unlabeled protein, and the total protein concentration was made up to 100 µM.

2.5 Liquid Droplet Formation

For all measurements, tau K18 droplets were formed upon incubation of 100 µM tau k18 with 0.5 mM TCEP in 50 mM sodium phosphate buffer of pH 8.8 at 37˚C.[29] Experiments were also carried with 100 µM tau k18 at pH 7.4 that resulted in droplet formation as well. Tau K18 did not form any droplets below 4˚C owing to its low critical solution transition behavior.[29] Liquid droplet formation was ensured by performing confocal microscopy in all the experiments.

2.6 Turbidity assay

Turbidity measurements were performed by recording optical density of 150 µL protein solutions (prepared in 50 mM sodium phosphate, 0.5 mM TCEP buffer of pH: 8.8) in 96-well optical bottom NUNC plate using Thermo Scientific Multiskan Go plate-reader instrument at 350 nm. All the data were recorded in triplets.

2.7 Confocal Microscopy

Labeled tau K18 was mixed with unlabeled fractions to make up the total concentration up to 100 µM. The protein solution was aliquoted into three sets for observing under the confocal microscope at different time points. About 5-6 µL of each aliquot was taken and placed over a clean glass slide (Fisher Scientific 3″ x 1″ x 1 mm) and then the drop of protein solution was mounted by a circular cover slip. At the two edges of the cover slip, nail paint was applied in order to seal it and prevent the evaporation of the solution. Images of the phase separated protein droplets were acquired using the Olympus FLUOVIEW confocal laser scanning microscope (Model no. FV10i) and a 60x oil-immersion objective (Numerical aperture: 1.35). The excitation sources used for visualizing the pyrene-1-maleimide, fluorescein-5-maleimide/AlexaFluor 488 C5-maleimide, and the AlexaFluor 594 C5-maleimide labeled droplets were the 405 nm (17.1 mW), 473 nm (11.9 mW), and 559 nm (15 mW) laser diodes, respectively, and the corresponding emission wavelengths were 461, 520, and 618 nm, respectively. The images were then imported and analyzed in the ImageJ software. (NIH, Bethesda, MD, USA).

2.8 Fluorescence quenching experiments with fluorescein-5-maleimide labeled tau k18:

Tau k18 was covalently labeled with fluorescein-5-maleimide (F5M) at the two cysteine residue positions, and solvent accessibility studies were performed in the presence of the water-soluble quencher potassium iodide (KI). 200 nM of the labeled protein was mixed with 99.8 µM unlabeled fractions and the mean fluorescence lifetime of the labeled protein was measured in the presence of increasing concentration of KI using Fluorocube (Horiba Jobin Yvon, NJ). The time-resolved fluorescence decays were also recorded simultaneously using TCSPC (Fluorocube, Horiba Jobin Yvon, NJ). The ratio of lifetime of F5M in the absence and presence of quencher was plotted against the quencher concentrations, and the bimolecular quenching constant was determined from the following equation:

$$\frac{\tau_0}{\tau} = 1 + K_{sv}[Q] \quad \textbf{(1)}$$

$$k_q = K_{sv}/\tau_0 \quad \textbf{(2)}$$

where, $\boldsymbol{\tau_0}$ and $\boldsymbol{\tau}$ are the fluorescence lifetimes of F5M in the absence and presence of the quencher KI, $\boldsymbol{K_{sv}}$ is the Stern-Volmer quenching constant, $[\boldsymbol{Q}]$ indicates the quencher concentration and $\boldsymbol{k_q}$ is the bimolecular quenching constant.

2.9. Steady-state fluorescence measurements:

All steady-state measurements were performed on a Fluoromax-4 (Horiba Jobin Yvon, NJ) spectrofluorimeter, using either 10 mm x 2 mm or 10 mm x 1 mm quartz cuvettes. F-5-M labeled and pyrene labeled samples were excited at 485 nm and 340 nm respectively. The steady-state fluorescence anisotropy (r_{ss}) data were also recorded at the respective emission maxima on the same instrument. The expression for the steady-state anisotropy is given by the following equation**:**

$$r_{ss} = \frac{I_{\parallel} - GI_{\perp}}{I_{\parallel} + 2GI_{\perp}} \qquad \textbf{(3)}$$

Where $I_{\parallel}$and $I_{\perp}$ represent the recorded fluorescence intensities when the emission polarizer is oriented parallel and perpendicular to the excitation polarizer, respectively, and the measured intensities were corrected using the corresponding G-factor values.

2.10. Time-resolved fluorescence measurements:

Picosecond time-resolved fluorescence measurements were carried out using the Fluorocube; Horiba Jobin–Yvon, N. time-correlated single photon counting (TCSPC) setup. The laser wavelength of 485 nm was used to excite the samples. The instrument response function was obtained using an aqueous solution of 2% ludox and was found to be ~ 270 ps. For fluorescence lifetime measurements, the fluorescence intensity decays were recorded at the magic angle (54.7˚) with 8 nm bandpass at the emission maxima. All the experiments were done at room temperature. The acquired intensity decays [I(t)] were fitted to bi-exponential decay kinetics.

$$I(t) = I_0 \left[\alpha_1 \, exp\left(-\frac{t}{\tau_1}\right) + \alpha_2 \, exp\left(-\frac{t}{\tau_2}\right)\right] \qquad \textbf{(4)}$$

Where, $\boldsymbol{I_0}$ is the time-zero intensity, $\boldsymbol{\alpha_1}$ and $\boldsymbol{\alpha_2}$ are the associated contributions of the lifetime components, $\boldsymbol{\tau_1}$ and $\boldsymbol{\tau_2}$.

The amplitude-weighted average mean fluorescence lifetimes were estimated using the following relationship:

$$< \tau > = \frac{\alpha_1 \tau_1^2 + \alpha_2 \tau_2^2}{\alpha_1 \tau_1 + \alpha_2 \tau_2} \quad \textbf{(5)}$$

The time-resolved fluorescence data were analyzed by a decay analysis program that was provided by Prof. N. Periasamy (Retd. TIFR Mumbai).

2.11. Formation of tau droplets in the presence of salt:

100 µM of tau K18 solution was prepared in the presence of 50, 100, 500 and 1000 µM of sodium chloride (NaCl) in 50 mM sodium phosphate, 0.5 mM TCEP buffer of pH: 8.8. Turbidity measurements of each solution (~150 µL) were carried out in Thermo Scientific Multiskan Go plate-reader instrument at 350 nm. Steady-state fluorescence depolarization measurements were performed using IAEDANS labeled tau K18.

3. Results and Discussion:

3.1 Conformational transition of tau K18 during phase separation:

Tau K18 has been found to phase separate in a variety of experimental conditions, including a wide range of pH (4.8-8.8), temperature (25˚C-42˚C), and protein concentrations (10 µM-100µM).[29] At high concentration of the protein and low temperature (below 15˚C), tau K18 does not form droplets. Droplet formation reaches a maximum with increasing temperature and then there is a drop with further increase in temperature, indicating that it undergoes lower critical solution transition (LCST). The amino acid sequence of proteins has been shown to have a strong influence on the phase separation behavior of the protein. Polypeptide chain enriched in arginine, such as FUS, is associated with UCST (upper critical solution transition) behavior or in other words, it phase separates below a certain critical temperature.[29] However, the high content of lysine in the amino acid sequence leads to LCST behavior. The repeat region of tau is enriched in lysine and thus confirms its association with LCST.[29] As a prelude, we first wanted to establish that tau K18 forms liquid-like droplets in our experimental conditions. When tau K18 was incubated at 37˚C under reducing condition (0.5 mM TCEP) at pH: 8.8, it formed mesoscopic spherical droplets after ~72 hr, which fused to form larger droplets when they come in contact with each other (**Figure 2**).

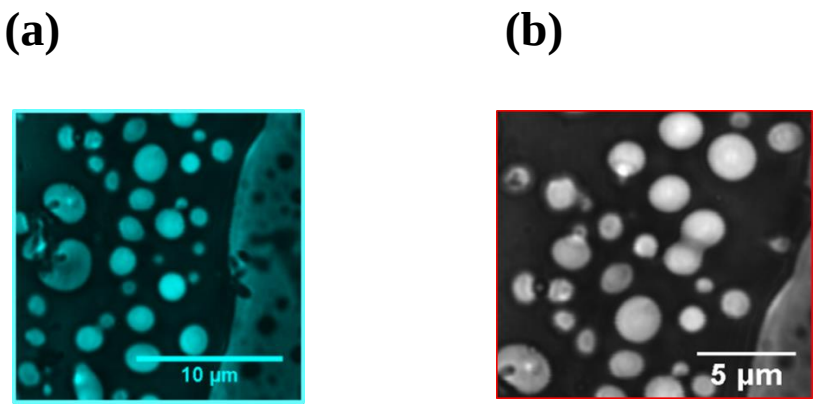

Figure 2. (a) An image of pyrene-labeled tau K18 droplets (b) An image of droplets showing fusion event.

Tau K18 exists as an ensemble of conformers with a preference to collapse in a structure in the presence of water, which is predicted by the PONDR plot (**Figure 3**).[35]

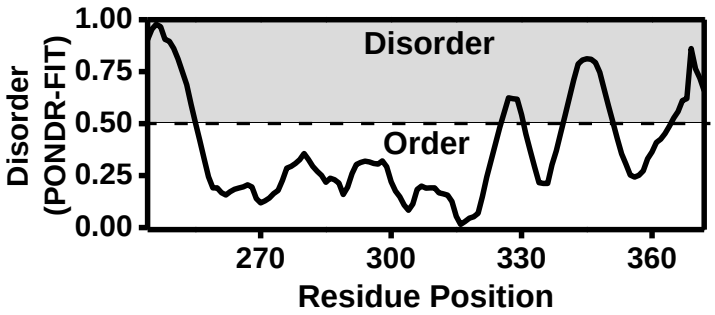

Figure 3. PONDR plot predicting disorder in the tau K18 sequence generated using (http://www.pondr.com/) and plotted using OriginPro 8.5.1 software.

So, after confirming that tau K18 forms liquid-like droplets at our experimental conditions, we asked the following question, does tau K18 undergoes a conformational change upon phase separation? To answer the question, we took advantage of the two native cysteines present in the repeat region of tau K18 and covalently labeled them with an intramolecular proximity probe, pyrene-maleimide.

The fluorescence emission spectrum of pyrene is characterized by 5 major vibrionic bands which are collectively known as the monomer bands. An interesting feature of pyrene fluorescence emission is that when two pyrene moieties are ~10 Å away from each other, then they form excited state dimer or excimer which gives rise to a long wavelength emission band.[36-38] Pyrene has an exceptionally long lifetime and thus permits the formation of such an excimer complex. Monomer bands are generated due to the return of an excited state monomer to its ground state. However, the excited state monomer can interact with a ground state monomer and form an excimer, or a ground state monomer can also interact with another ground state monomer to generate a dimer which upon excitation gives rise to an excimer and thus gives an excimer band.[38] This unique feature of pyrene fluorescence we chose pyrene maleimide as a probe for our experiments.

We labeled tau K18 with pyrene-maleimide and mixed 1 µM of the labeled protein with 99 µM of unlabeled tau K18. The protein solution was incubated at 37˚C, and the fluorescence characteristics of pyrene-labeled tau K18 was observed over time. At the monomer state, a

long wavelength excimer band was observed indicating that the two pyrene moieties are in close proximity with each other (**Figure 4a**). This observation was also in good agreement with the PONDR plot of tau K18 discussed above. Upon phase separation (after ~48 hrs), the excimer band intensity dropped pointing toward the possibility that the pyrene moieties might be moving away from each other, or in other words, the polypeptide chain adopts an extended conformation (**Figure 4a**).

(a)

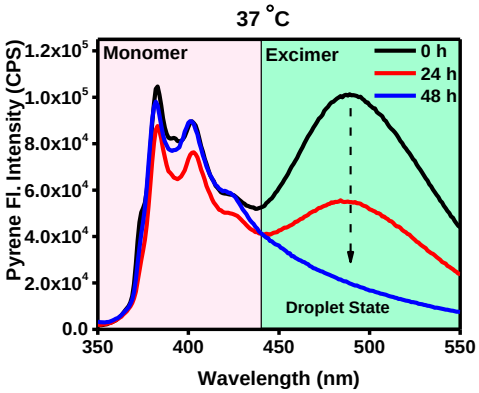

(b)

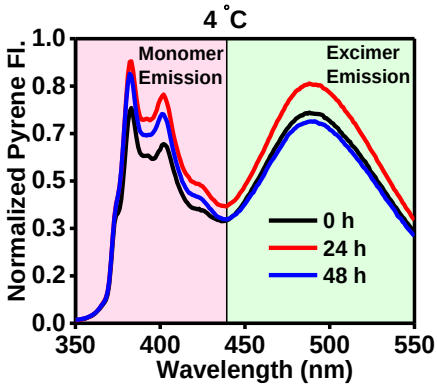

(c)

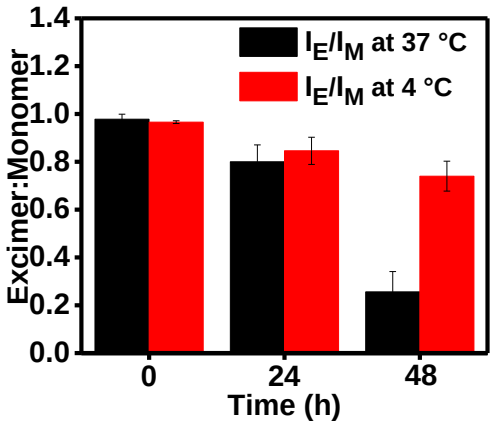

(d)

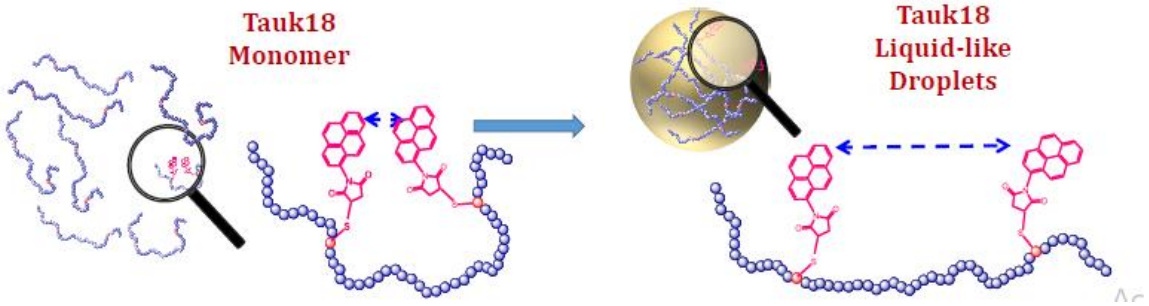

Figure 4. (a) Emission spectra of pyrene-labeled tau K18 at 37˚C. (b) Emission spectra of pyrene-labeled tau K18 at 4˚C. (c) Excimer-to-monomer ratio of emission spectra of pyrene-labeled tau K18 at 37˚C and 4˚C. (d) Schematic representation of the unraveling of the polypeptide chain upon phase separation. (Image courtesy: Dr. Anupa Majumdar, a National Post-Doctoral Fellow in our lab)

In order to confirm that the decrease in excimer fluorescence intensity is due to phase separation, we performed control experiments at 4˚C. Since tau K18 has been known to undergo LCST, so 4˚C was chosen as the temperature for performing control experiment, at which no droplets will be formed.[29] Upon incubation at 4˚C, no significant drop in excimer fluorescence intensity was observed with time, which confirmed our previous observation that tau K18 undergoes a change in its conformation, from a collapsed polypeptide chain to an extended coil (**Figure 4b**). The polypeptide chains can act as its own good solvent inside the droplets which enable the unraveling of the chains to form a multitude of intermolecular cross-talks between the polypeptide chains favoring phase separation. This structural interpretation led us to some important questions: (a) does the droplet interior recruit water? (b) Is there any change in the conformational dynamics of the polypeptide chains within the droplets?

3.2 Solvent accessibility of tau K18 inside the droplets:

We wanted to probe the solvent environment inside the phase separated droplets. In order to do that, we labeled tau K18 with fluorescein-5-maleimide and mixed 200 nM of the labeled protein with 99.8 µM of unlabeled fractions. Solvent accessibility studies were performed by doing Stern-Volmer quenching experiments of fluorescein-labeled tau K18

in the presence of a water-soluble quencher, potassium iodide (KI).[36] The fluorescence lifetimes of fluorescein-labeled protein and free fluorescein were obtained both in the absence of the quencher as well as in the presence of increasing amount of the quencher. The fluorescence lifetime data collected was plotted against the increasing concentrations of KI, and the plot revealed that free fluorescein had the steepest slope, following which were the slopes of the curves of phase separated tau K18 and monomer tau K18 in the order of decreasing steepness (**Figure 5**).

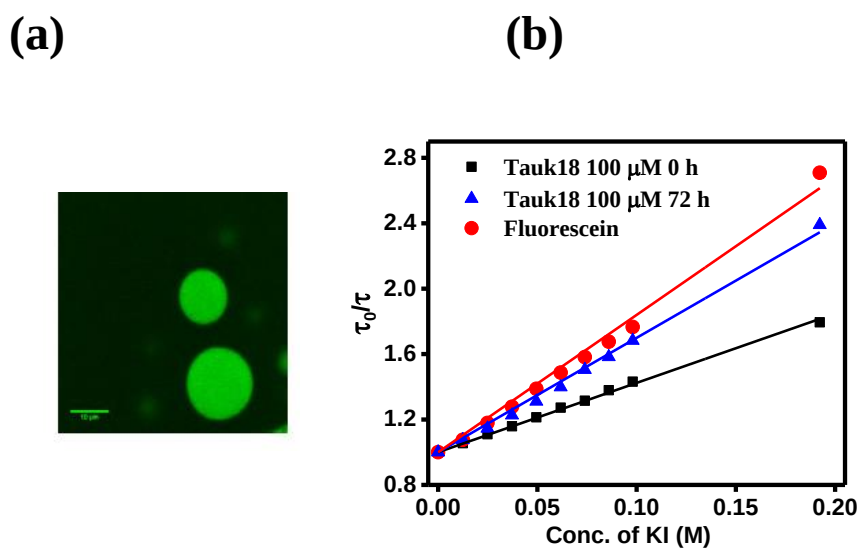

Figure 5. (a) An image of fluorescein-labeled tau K18 droplets. (b) Stern-Volmer plots of free fluorescein, monomeric tau K18 (0 hr) and tau K18 droplets (72 hrs) by plotting mean fluorescence lifetime in the absence and presence of KI.

The Stern-Volmer quenching constant and the bimolecular rate constant were also derived for free fluorescein, monomer and phase separated protein from the lifetime measurements which are stated in the table below (**Table 1**).

Table 1. Values of the recovered Stern–Volmer constants (K_{SV}) obtained from fitting the plots shown in **Figure 4** using **equation (1)** and the calculated bimolecular quenching constants (k_q) obtained using **equation (2)**.

Sample	**τ_0 (ns)**	**K_{sv} (M^{-1})**	**k_q ($M^{-1}s^{-1}$)**
Free Fluorescein	3.94 ± 0.01	8.39 ± 0.18	(2.1 ± 0.04) x 10^9
Tau K18 Monomer	4.01 ± 0.03	4.24 ± 0.04	(1.1 ± 0.01) x 10^9
Tau K18 Droplet	3.91 ± 0.01	6.99 ± 0.10	(1.8 ± 0.03) x 10^9

The results revealed that free fluorescein exhibits the highest degree of water accessibility as indicated by a steeper slope. Tau K18 in the monomer state exhibits less accessibility to water due to its compact conformation. However, in the droplet state solvent accessibility is higher which suggests that these protein-rich droplets are not water excluded. Moreover, we also recorded fluorescence emission spectra of acrylodan labeled tau K18. Acrylodan being an environment sensitive dye gives information regarding the local environment of the dye. It was observed that upon phase separation, there is a red-shift in the emission maximum of acrylodan labeled tau K18 (**Figure 6**).

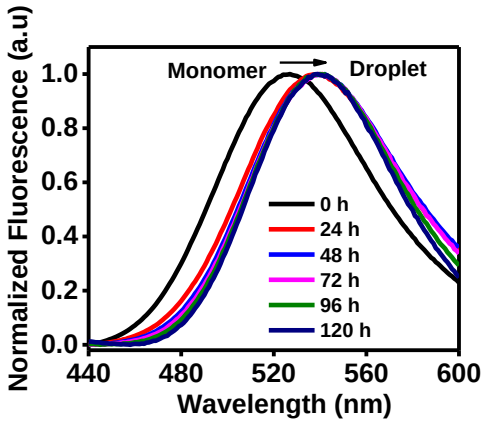

Figure 6. Fluorescence emission spectra of acrylodan labeled tau K18 showing a red-shift as a function of increased droplet formation.

These results indicate that there is significant chain solvation inside the droplets. The mesoscopic spherical droplets formed upon phase separation recruit a considerable amount

of water inside them raising the possibility that the droplet interior might resemble a semi-dilute regime. The solvent environment inside the droplets is dictated by the coexistence of several protein chains and water molecules which renders the droplet interior more analogous to a polar organic solvent. Such a solvent environment is more favorable for the expansion or unraveling of the polypeptide chains within the droplets. These extended polypeptide chains may undergo transient intermolecular interactions and thus, we next looked at the dynamics of the polypeptide chains inside the droplets.

3.3 Phase separation is associated with decrease in anisotropy:

We wanted to know whether tau K18 undergoes any change in conformational dynamics upon phase separation. In order to do that, we labeled tau K18 with fluorescein-5-maleimide and mixed 200 nM of the labeled protein with 99.8 µM of unlabeled tau K18 to study fluorescence depolarization kinetics of fluorescein-labeled tau K18. We first performed steady-state anisotropy measurements of fluorescein-labeled tau K18. Fluorescence anisotropy is related to the rotational flexibility of a molecule. A small dye molecule tumbles faster and thus exhibits a low anisotropy, whereas when the dye molecule is attached to a large macromolecule, it experiences restricted motion, thereby exhibits higher anisotropy.[33,36] Interestingly, we observed that the steady-state anisotropy values of fluorescein-labeled tau K18 upon phase separation was much lower compared to the monomeric state of tau K18 (**Figure 7**).

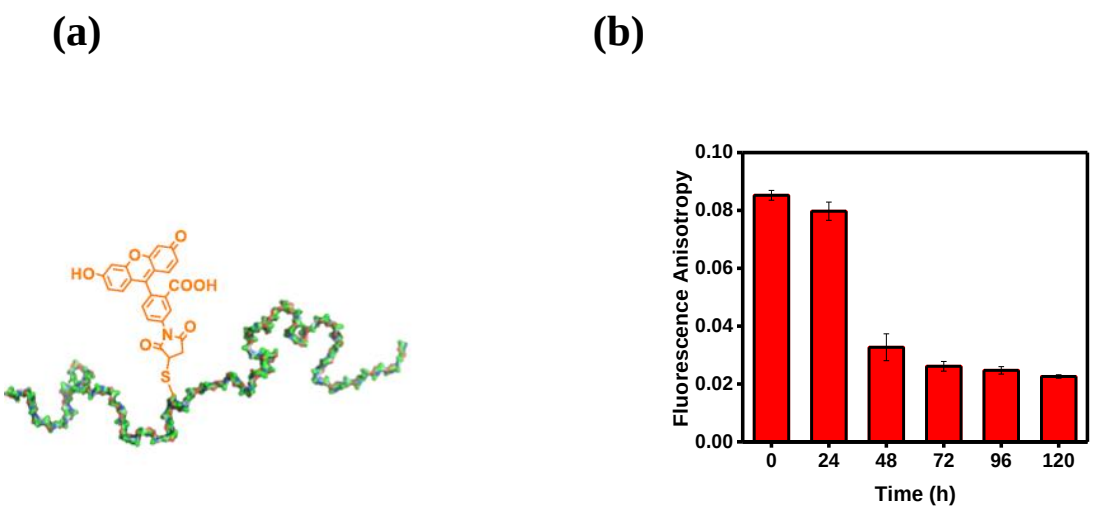

Figure 7. (a) Schematic representation of fluorescein-labeled tau K18. (b) Steady-state fluorescence anisotropy of fluorescein-labeled tau K18 as a function of time during droplet formation.

Since anisotropy is also affected by the degree of turbidity of the solution, we performed similar experiments with diluted solutions as well. The steady-state anisotropy values of the dilute solutions remained unaltered, indicating that the decrease in anisotropy values was due to increased mobility of the polypeptide chains (**Figure 8**).

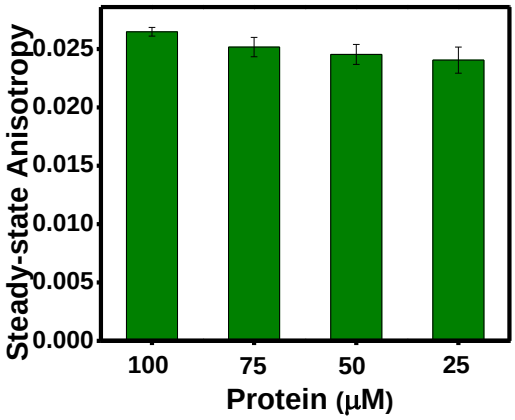

Figure 8. Steady-state fluorescence anisotropy of fluorescein-labeled tau K18 recorded as a function of serial dilution of the droplets formed after 72 h.

Next, we conducted a control experiment at 4˚C in order to confirm that the decrease in anisotropy values was indeed due to droplet formation. Tau K18 does not undergo phase separation at low temperature due to its LCST behavior, and thus 4˚C was chosen as the temperature for performing the control experiment. It was observed that the steady-state anisotropy values remained constant even after 48 hrs of incubation at 4˚C (**Figure 9**).

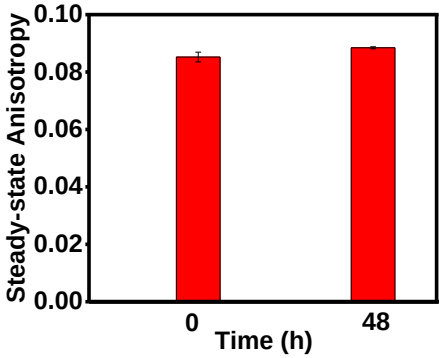

Figure 9. No decrease in the fluorescence anisotropy of fluorescein-labeled tau K18 was observed after incubating at 4 °C that does not result in droplet formation.

We also performed similar experiments with another fluorophore named iaedans. We labeled tau K18 with iaedans and conducted steady-state anisotropy experiments in the monomeric, and the phase separated state (**Figure 10**). The data revealed a similar decrease in anisotropy values as was observed in the case of fluorescein-labeled tau K18.

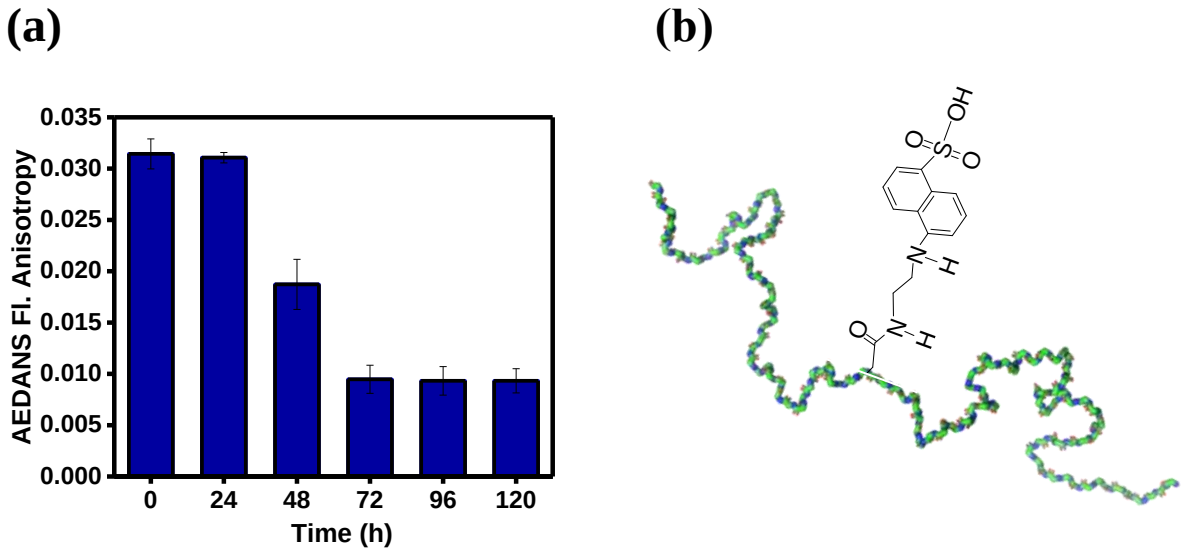

Figure 10. (a) Steady-state fluorescence anisotropy of IAEDANS-labeled tau K18 as a function of time during droplet formation. (b) Schematic representation of IAEDANS labeled tau K18.

These results suggest that the decrease in anisotropy values is due to the formation of phase-separated droplets and the polypeptide chains experience a high degree of flexibility inside the droplets. Next, in order to further confirm the association of phase separation with decrease in anisotropy, we performed similar experiments in presence of salts.

3.4 Effect of ionic strength on phase separation behavior:

Phase separation of many proteins, enriched in charged residues has been found to depend on the ionic strength of the surrounding environment.[30] Tau K18 is rich in positively charged lysine residues, and thus we wanted to observe how changes in the ionic strength affect its phase separation behavior. In order to do that, we observed the variation in turbidity and steady-state anisotropy values with increasing concentrations of sodium chloride. Turbidity values collected at 350 nm were similar for all solutions containing different concentrations of sodium chloride. However, after 72 hrs, the turbidity of the solutions containing 0, 50 and 100 mM sodium chloride increased and that of the solutions

containing 500 and 1000 mM sodium chloride remained almost unaltered (**Figure 11**). This result revealed that phase separation behavior of tau K18 was not affected by the increasing salt concentration up to 500 mM sodium chloride, or in other words, high salt concentrations are required to shield the electrostatic interactions among the polypeptide chains for tau K18 phase separation.

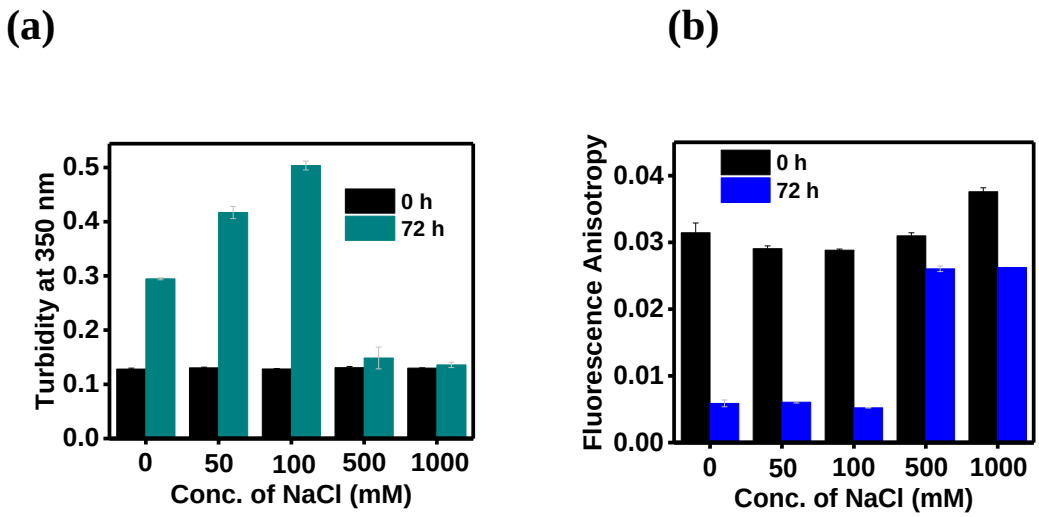

Figure 11. (a) Changes in turbidity in the monomer and droplet state of tau K18 with increasing concentrations of NaCl, measured at 350 nm. (b) Changes in the steady-state anisotropy in the monomer and droplet state of tau K18 with increasing concentrations of NaCl.

Similar observations were made in case of fluorescence depolarization experiments as well. The steady-state anisotropy values were decreased considerably compared to the initial anisotropy values in case of solutions containing 0, 50 and 100 mM of sodium chloride but remained almost same in the solutions containing higher salt concentrations, which further confirmed our previous conclusion that phase separation of tau K18 is associated with the decrease in anisotropy values.

3.5. Enhanced conformational dynamics of the polypeptide chains within the droplets:

Steady-state anisotropy gives average information of the immediate microenvironment of the dye and does not differentiate the conformational dynamics of the protein or different motions in the protein that contribute towards depolarization of fluorescence. However, ultra-sensitive picosecond time-resolved anisotropy can discern the different molecular

events that are responsible for fluorescence depolarization.[33,36] The fluorescence depolarization kinetics is described by a bi-exponential decay function, consisting of φ_{fast} which corresponds to the local mobility of the fluorophore attached to a polypeptide chain and φ_{slow} which corresponds to the global motion of the protein.[33,36] When any dye is attached to a bio macromolecule, there are two possible modes of motion that contribute towards depolarization in case of proteins, the local motion associated with the tumbling of the dye along its axis and global motion due to the overall tumbling of the protein. Our previous studies have shown that φ_{slow} represents the overall tumbling of the protein in case of compact globules depending on its hydrodynamic volume, but in case of IDPs it corresponds to a size-independent characteristic timescale (~1.3 ns) that arises due to segmental torsional mobility of the Ramachandran Φ –Ψ dihedral angles of the expanded polypeptide chains (**Figure 12**).[33,36]

(a)

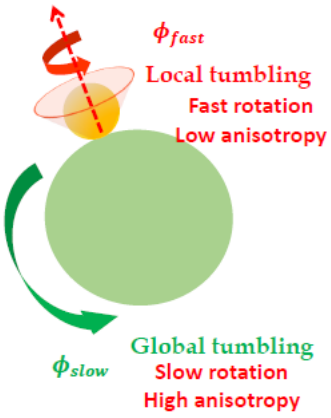

(b)

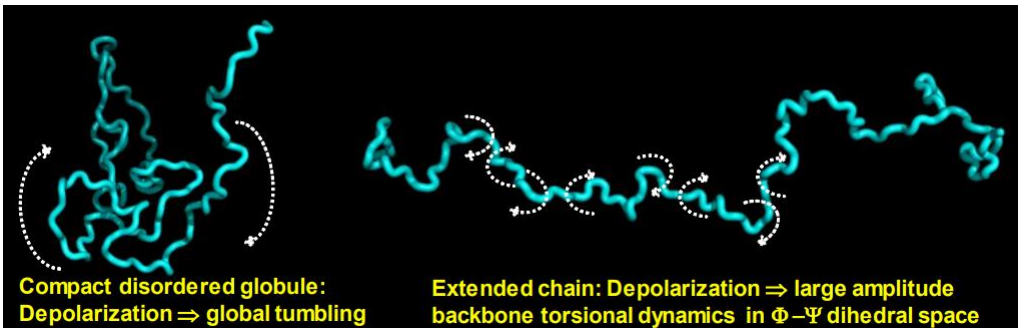

Figure 12. (a) Schematic representation of the local motion of a dye molecule and the global tumbling of the protein. (b) Schematic representation of the global motion of a compact globule and the torsional mobility of the polypeptide backbone. (Image courtesy: Dr. Anupa Majumdar and Dr. Samrat Mukhopadhyay)

We performed time-resolved anisotropy measurements of fluorescein-labeled tau K18 using procedure as mentioned previously[33] (**Figure 13**). Upon fitting the decay curves to bi-exponential decay function, we recovered the parameters φ_{fast} and φ_{slow} corresponding to fluorescein labeled tau K18 both in the monomer and droplet state. The values of the recovered parameters have been listed below (**Table 2**).

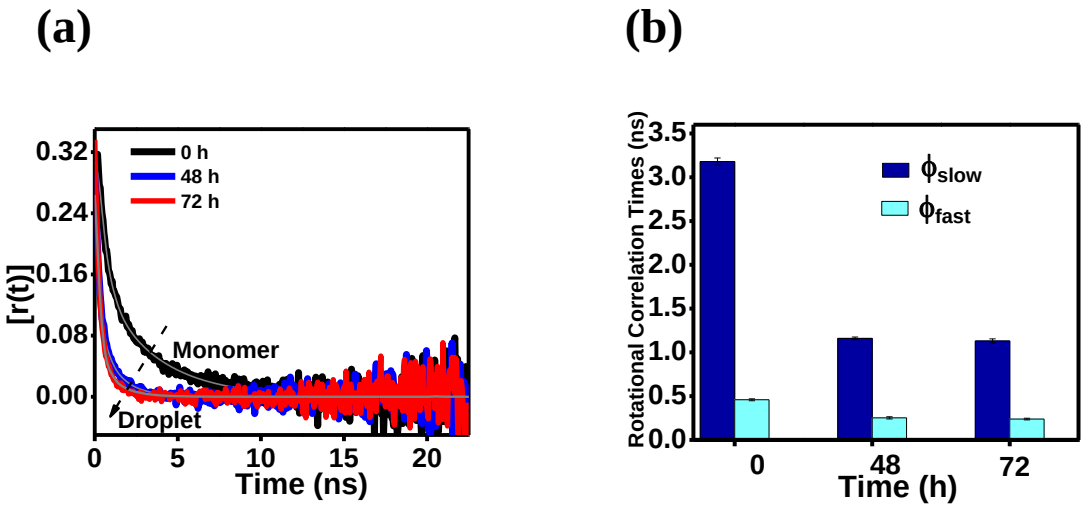

Figure 13. (a) Time-resolved fluorescence anisotropy decays. The black lines are the fits using bi-exponential decay kinetics of depolarization. (b) Changes in rotational correlation times along with the standard deviation for three independent measurements. (All time-resolved anisotropy experiments were performed and the data were analyzed by Dr. Anupa Majumdar, a national postdoctoral fellow in our lab.)

Table 2. The typical parameters recovered from fitting of the fluorescence anisotropy decay profiles shown in **Figure 13**(a).

Sample	r_0	Φ_{fast} (ns)	β_{fast}	Φ_{slow} (ns)	β_{slow}
Tau K18 monomer (0 h)	0.32 ± 0.002	0.46 ± 0.01	0.52 ± 0.004	3.18 ± 0.04	0.48 ± 0.004
Tau K18 Droplets (48 h)	0.34 ± 0.008	0.25 ± 0.01	0.72 ± 0.005	1.16 ± 0.01	0.28 ± 0.005
Tau K18 Droplets (72 h)	0.34 ± 0.03	0.24 ± 0.01	0.87 ± 0.003	1.13 ± 0.02	0.13 ± 0.007

It was observed that the value of was ~3 ns in the monomeric state of tau K18 and ~1.1 ns in the droplet state which pointed toward much faster depolarization kinetics in the droplet state. This decrease in the value of slow rotational correlation time suggests that upon phase separation, the extended polypeptide chains undergo rapid dihedral rotations on a timescale close to the backbone torsional relaxation expected for expanded chains in good solvents. Thus, the expanded polypeptide chains undergo rapid conformational fluctuations inside the phase separated droplets which in turn help them to maintain the liquid-like characteristics of the droplets.

4. Conclusion and Future Direction:

A lot of research has been carried out recently in determining the link between the amino acid sequence of a protein and its phase separation behavior, but the molecular mechanism underlying liquid-liquid phase separation remains poorly understood.[10,11] Here, using a wide range of biophysical and optical tools we were able to capture some interesting molecular events during the course of phase separation of an intrinsically disordered protein named tau. We worked with the repeat region of tau because it has the ability to modulate the propensity of tau to aggregate. Using an intramolecular proximity readout, we were able to show the unraveling of the polypeptide chain upon phase separation of tau K18 which is essential for forming intermolecular crosslinks between the polypeptide chains through a multitude of non-covalent interactions. The solvent accessibility studies revealed that water is present inside the phase separated droplets which helps in the solvation of the polar and charged residues present in the polypeptide chain. Presence of a significant amount of water inside the droplets has led us to characterize them as semi-dilute. The chain solvation aids in the rapid fluctuation of the chains and thereby helps in maintaining the fluidity of the liquid-like droplets. The repeat regions of tau K18 is enriched in PGGG domains which might also act as linkers between the sticky domains and favor enhanced chain fluctuations.[39] Ultra-sensitive picosecond time-resolved fluorescence depolarization experiments directly showed the rapid large-scale fluctuations of the expanded polypeptide chains. The rapid conformational fluctuations can temporally control the making and the breaking of intermolecular, noncovalent interactions between the "stickers" of the polypeptide chains on a characteristic timescale which can further enable reformation of the new contacts with other polypeptide chains inside the droplets. The making and the breaking of the contacts can be crucial for maintaining the liquid-like property of the droplets. The unraveling of the chain, solvation of the polar and charged residues in the polypeptide chain along with rapid chain fluctuations promote a variety of intermolecular transient non-covalent interactions that are crucial for tau K18 to undergo phase separation. This work can further be extended in identifying regions of the polypeptide chain involved in liquid-liquid phase separation of tau K18. One can also try to understand in greater depth how exactly the chain dynamics favor the phase separation and also try to quantify the timescales of the transient intermolecular interactions.

5. Bibliography

1. Shin Y, Brangwynne CP (2017) Liquid Phase Condensation in Cell Physiology and Disease. Science 357: eaaf4382:1-11.
2. Hyman AA, Weber CA, Jülicher F (2014) Liquid-Liquid Phase Separation in Biology. Annu. Rev. Cell Dev. Biol. 30: 39–58.
3. Franzmann TM, Jahnel M, Pozniakovsky A, Mahamid J, Holehouse AS, Nüske E, Richter D, Baumeister W, Grill SW, Pappu RV, Hyman AA, Albert S (2018) Phase Separation of a Yeast Prion Protein Promotes Cellular Fitness. Science 359: eaao5654:1-8.
4. Shorter J (2016) Membraneless Organelles: Phasing in and Out. Nat. Chem. 8: 528-530.
5. Feric M, Vaidya N, Harmon TS, Mitrea DM, Zhu L, Richardson TM, Kriwacki RW, Pappu RV, Brangwynne CP (2016) Coexisting Liquid Phases Underlie Nucleolar Subcompartments. Cell 165: 1686-1697
6. Uversky VN (2017) Intrinsically Disordered Proteins in Overcrowded Milieu: Membrane-Less Organelles, Phase Separation, and Intrinsic Disorder. Curr. Opin. Struct. Biol. 44: 18-30.
7. Wei MT, Elbaum-Garfinkle S, Holehouse AS, Chen CCH, Feric M, Arnold CB, Priestley RD, Pappu RV, Brangwynne CP (2017) Phase Behaviour of Disordered Proteins Underlying Low Density and High Permeability of Liquid Organelles. Nat. Chem. 9: 1118–1125.
8. Elbaum-Garfinkle S, Kim Y, Szczepaniak K, Chen CC-H, Eckmann CR, Myong S, Brangwynne CP (2015) The Disordered P Granule Protein LAF-1 Drives Phase Separation into Droplets with Tunable Viscosity and Dynamics. Proc. Natl. Acad. Sci. U. S. A. 112: 7189-94.
9. Posey AE, Holehouse AS, Pappu RV (2018) Phase Separation of Intrinsically Disordered Proteins. Methods Enzymol. 611: 1-30.
10. Martin EW, Mittag T (2018) Relationship of Sequence and Phase Separation in Protein Low-Complexity Regions. Biochemistry 57: 2478-2487.
11. Pak CW, Kosno M, Holehouse AS, Padrick SB, Mittal A, Ali R, Yunus AA, Liu DR, Pappu RV, Rosen MK (2016) Sequence Determinants of Intracellular Phase Separation by Complex Coacervation of a Disordered Protein. Mol. Cell 63: 72-85.

12. Boeynaems S, Alberti S, Fawzi N L, Mittag T, Polymenidou M, Rousseau F, Schymkowitz J, Shorter J, Wolozin B, Van Den Bosch L, Tompa P, Fuxreiter M (2018) Protein Phase Separation: A New Phase in Cell Biology. Trends Cell Biol. 28: 420-435.
13. Habchi J, Tompa P, Longhi S, Uversky VN (2014) Introducing Protein Intrinsic Disorder. Chem. Rev. 114: 6561–6588.
14. Uversky VN (2011) Intrinsically disordered proteins from A to Z. Int. J. Biochem. Cell Biol. 43: 1090-1103.
15. Rocha EM, Miranda BD, Sanders LH (2018) Alpha-synuclein: Pathology, mitochondrial dysfunction and neuroinflammation in Parkinson's disease. Neurobiol. Dis. 109: 249-257.
16. Ballatore C, Lee VM, Trojanowski JQ (2007) Tau-mediated neurodegeneration in Alzheimer's disease and related disorders. Nat. Rev. Neurosci. 8: 663-672.
17. Udagawa T, Fujioka Y, Tanaka M, Honda D, Yokoi S, Riku Y, Ibi D, Nagai T, Yamada K, Watanabe H, Katsuno M, Inada T, Ohno K, Sokabe M, Okado H, Ishigaki S, Sobue G (2015) FUS regulates AMPA receptor function and FTLD/ALS-associated behaviour via GluA1 mRNA stabilization. Nat. Commun. 6: 7098
18. Daldin M, Fodale V, Cariulo C, Azzolini L, Verani M, Martufi P, Spiezia MC, Deguire SM, Cherubini M, Macdonald D, Weiss A, Bresciani A, Vonsattel JPG, Petricca L, Marsh JL, Gines S, Santimone I, Marano M, Lashuel HA, Squitieri F, Caricasole A (2017) Polyglutamine expansion affects huntingtin conformation in multiple Huntington's disease models. Sci. Rep. 7: 5070.
19. Protter DSW, Rao BS, Van Treeck B, Lin Y, Mizoue L, Rosen MK, Parker R (2018) Intrinsically Disordered Regions Can Contribute Promiscuous Interactions to RNP Granule Assembly. Cell Rep. 22: 1401-1412.
20. Ryan VH, Dignon GL, Zerze GH, Chabata CV, Silva R, Conicella AE, Amaya J, Burke KA, Mittal J, Fawzi NL (2018) Mechanistic View of hnRNPA2 Low-Complexity Domain Structure, Interactions, and Phase Separation Altered by Mutation and Arginine Methylation. Mol. Cell 69: 465-479.
21. Mitrea DM, Cika JA, Stanley CB, Nourse A, Onuchic PL, Banerjee PR, Phillips AH, Park CG, Deniz AA, Kriwacki RW (2018) Self-Interaction of NPM1 Modulates Multiple Mechanisms of Liquid-Liquid Phase Separation. Nat. Commun. 9:1-13.

22. Brangwynne CP, Tompa P, Pappu RV (2015) Polymer physics of intracellular phase transitions. Nat. Phys. 11: 899-904.
23. Langdon EM, Qiu Y, Niaki AG, McLaughlin GA, Weidmann CA, Gerbich TM, Smith JA, Crutchley JM, Termini CM, Weeks KM, Myong S, Gladfelter AS (2018) mRNA Structure Determines Specificity of a PolyQ-Driven Phase Separation. Science 360: 922-927.
24. Dzuricky M, Roberts S, Chilkoti A (2018) Convergence of Artificial Protein Polymers and Intrinsically Disordered Proteins. Biochemistry 57: 2405-2414.
25. Melo AM, Elbaum-Garfinkle S, Rhoades E (2017) Insights into tau function and dysfunction through single-molecule fluorescence. Methods Cell Biol. 141: 27-44.
26. Elbaum-Garfinkle S, Rhoades E (2012) Identification of an Aggregation-Prone Structure of Tau. J. Am. Chem. Soc. 134: 16607-16613.
27. Eschmann NA, Georgieva ER, Ganguly P, Borbat PP, Rappaport MD, Akdogan Y, Freed JH, Shea JE, Han S (2017) Signature of an Aggregation-Prone Conformation of Tau. Sci. Rep. 7: 44739:1-10.
28. Ramachandran G, Udgaonkar JB (2013) Mechanistic Studies Unravel the Complexity Inherent in Tau Aggregation Leading to Alzheimer's Disease and the Tauopathies. Biochemistry 52: 4107-4126.
29. Ambadipudi S, Biernat, J, Riedel D, Mandelkow E, Zweckstetter M (2017) Liquid-Liquid Phase Separation of the Microtubule-Binding Repeats of the Alzheimer-Related Protein Tau. Nat. Commun. 8: 275:1-13.
30. Wegmann S, Eftekharzadeh B, Tepper K, Zoltowska KM, Bennett RE, Dujardin S, Laskowski PR, MacKenzie D, Kamath T, Commins C, Vanderburg C, Roe AD, Fan Z, Molliex AM, Hernandez-Vega A, Muller D, Hyman AA, Mandelkow E, Taylor JP, Hyman BT (2018) Tau Protein Liquid–liquid Phase Separation Can Initiate Tau Aggregation. EMBO J. 37: e98049:1-21.
31. Hernández-Vega A, Braun M, Scharrel L, Jahnel M, Wegmann S, Hyman BT, Alberti S, Diez S, Hyman AA (2017) Local Nucleation of Microtubule Bundles through Tubulin Concentration into a Condensed Tau Phase. Cell Rep. 20: 2304-2312.
32. Bhasne K, Sebastian S, Jain, N, Mukhopadhyay S (2018) Synergistic Amyloid Switch Triggered by Early Heterotypic Oligomerization of Intrinsically Disordered α-Synuclein and Tau. J. Mol. Biol. 430: 2508-2520.

33. Majumdar A, Mukhopadhyay S (2018) Fluorescence Depolarization Kinetics to Study the Conformational Preference, Structural Plasticity, Binding, and Assembly of Intrinsically Disordered Proteins. Methods Enzymol. 611, 347-382.
34. Jain N, Narang D, Bhasne K, Dalal V, Arya S, Bhattacharya M, Mukhopadhyay S (2016) Direct Observation of the Intrinsic Backbone Torsional Mobility of Disordered Proteins. Biophys. J. 111:768–774.
35. Xue B, Dunbrack RL, Williams RW, Dunker AK, Uversky VN (2010) PONDR-FIT: A Meta-Predictor of Intrinsically Disordered Amino Acids. Biochim. Biophys. Acta. 1804: 996- 1010.
36. Lakowicz JR (2006) Principles of Fluorescence Spectroscopy, 3rd Ed. (Springer, New York).
37. Jain N, Bhattacharya M, Mukhopadhyay S (2011) Chain Collapse of an Amyloidogenic Intrinsically Disordered Protein. Biophys. J. 101: 1720-1729.
38. Bains G, Patel AB, Narayanaswami V (2011) Pyrene: A Probe to Study Protein Conformation and Conformational Changes. Molecules 16: 7909-7935.
39. Wang J, Choi J–M, Holehouse AS, Lee HO, Zhang X, Jahnel M, Maharana S, Lemaitre R, Pozniakovsky A, Drechsel D, Poser I, Pappu RV, Alberti H, Hyman AA (2018) A Molecular Grammar Governing the Driving Forces for Phase Separation of Prion-like RNA binding proteins. Cell 174: 688-699.